Experimental Investigation, Application and Monitoring of a Simple for Dead Load–Continuous for Live Load Connection for Accelerated Modular Steel Bridge Construction

SAEED JAVIDI, AARON YAKEL and ATOROD AZIZINAMINI

ABSTRACT

The inherently modular nature of the simple for dead–continuous for live load system (SDCL) makes it a natural fit for the accelerated construction paradigm. A detail capable of connecting pre-topped girders over the middle supports is developed and described in this paper. To evaluate the performance of the proposed connection, a full-scale specimen was built and subjected to cyclic and ultimate load testing. The connection showed very little change during cyclic loading equivalent for 70 years of traffic. During the ultimate load test, the connection demonstrated large displacement ductility, reaching its ultimate capacity after complete yielding of the longitudinal reinforcement. After the successful experimental test, a field application bridge was constructed utilizing a modular pre-topped steel box girder system, which allows much of the construction process to be performed prior to placing the girders. The bridge consisted of three pre-topped steel box units placed side by side and connected using longitudinal joints between pre-topped units. The steel box girders used 70-ksi high-performance steel in the bottom flange and 50-ksi steel in the top flanges and webs. The use of high-performance steel combined with the simple for dead–continuous for live load system allows eliminating the need for section transitions through the length of the structure and using constant cross-section throughout the length of the girders. Long-term monitoring of the structure was performed and showed the system performed as intended.

Keywords: steel bridges, steel girders, SDCL, simple for dead load–continuous for live load.

INTRODUCTION

This paper provides description of the development and implementation of the simple for dead–continuous for live loads (SDCL) bridge system for steel girders, a method well suited for accelerated bridge construction (ABC). The SDCL bridge system employs a joint detail at the interior supports that does not become continuous until after the dead loads have been applied. Prior to attaining this final continuity, the girders within the individual spans are simply supported. General information regarding the behavior and design of the SDCL system can be found in a companion series paper by Azizinamini (2014).

A current trend in bridge construction is the adoption of accelerated construction practices that reduce onsite construction time to mitigate extended disruptions to traffic. The inherently modular nature of the SDCL system makes it a natural fit for the accelerated construction paradigm. Therefore, the research being presented in this paper extends the simple-made-continuous system to address modular bridge construction methods. In addition to accelerating the bridge construction process, the system presented also greatly enhances worker safety.

Saeed Javidi, Ph.D., P.Eng., Structural Engineer, Associated Engineering Ltd., Burnaby, BC, Canada. Email: sjavidin@gmail.com

Aaron Yakel, Ph.D., Research Associate, Civil and Environmental Engineering Department, Florida International University, Miami, FL. Email: ayakel@fiu.edu

Atorod Azizinamini, Ph.D., P.E., Professor and Chair, Civil and Environmental Engineering Department, Florida International University, Miami, FL (corresponding). Email: aazizina@fiu.edu

RESEARCH OBJECTIVES AND SCOPE

The simple for dead–continuous for live load concept has been used with prestressed concrete bridges for many years. Research conducted at the University of Nebraska–Lincoln extends the application of this system to steel girder bridges.

The key component in the simple for dead load made continuous for live load system is the continuity connection over the interior supports. For the purpose of extending the application of SDCL system to bridges constructed using principles of accelerated bridge construction, detail capable of connecting the pre-topped girders over the middle supports is developed and described in this paper. To evaluate the performance of the proposed connection, a full-scale specimen was built and various tests conducted. The specimen was representative of the negative flexure region of a

two-span bridge having 94-ft span lengths with four girders, spaced at 8 ft 4 in. The tests carried out included static and cyclic loading to comprehend the strength and fatigue performance of the detail and development of appropriate design provisions. The results of the cyclic and ultimate test are described, and the load-resistance mechanism of the connection is examined. Following the completion of the experimental testing, the detail was utilized in the construction of the 262nd Street Bridge over I-80 in Nebraska. Several innovative concepts were used in the construction of this bridge. The bridge was instrumented and monitored during service for more than 2 years. Design and construction of the 262nd Street Bridge demonstrated the feasibility of using the developed detail in practice.

SYSTEM DESCRIPTION

Continuous steel bridges are usually constructed so that the system provides continuity for all loading, both dead and live. However, in SDCL steel bridge systems, girders behave as simply supported under their own self-weight and during casting of the concrete deck. The interior support connection detail is such that once the deck has been cast and allowed to cure, the system then becomes continuous for subsequent loading. The continuity for live loads is provided for by providing steel reinforcement over the interior support, before the casting deck.

Modular Concept

One of the objectives in using modular bridge systems is to minimize the interruption to traffic. This objective is achieved by casting the concrete deck over the girder, prior to placement over the supports. Pre-topped girders are then placed side by side and connected using narrow longitudinal joints. Figure 1 shows the system used for the 262nd Street Bridge, which incorporates SDCL, pre-topped and adjacent girder concepts.

The concept of pre-topped, adjacent girder system for ABC applications is also used with concrete girders. However, using steel girders provides two main advantages. First, the concrete girder with a pre-topped deck could weigh several times more than steel alternates. Second, concrete girders experience creep and shrinkage displacement, which creates challenges during construction. The creep and shrinkage displacement of pre-topped concrete girders results in pre-topped units to assume different elevations, which is difficult to correct in the field. This problem becomes more significant as girder length increases. Use of steel girders in a pre-topped, adjacent system, in large part, eliminates this challenging field problem, especially when a full-depth pre-topped deck system is used.

Pier Connection Detail

In the conventional SDCL system, continuous longitudinal reinforcement is placed over the interior support that is then

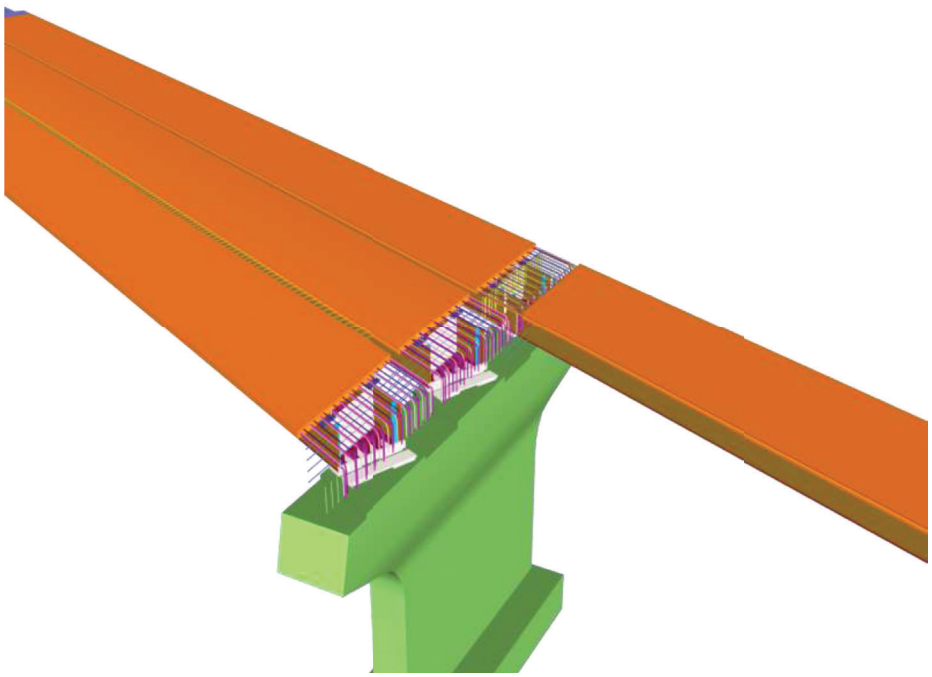

Fig. 1. Conceptual drawing of SDCL system using pre-topped and adjacent girder concepts.

cast into the deck. This is clearly not possible in the modular system because the concrete deck is already cast. Somehow the reinforcement from one span must be spliced with the reinforcement from the next span. The solution was to allow the longitudinal reinforcement to extend out of the concrete deck at the interior support. The reinforcement bars over the pier are then developed by hooking them in the concrete diaphragm. This detail can be seen in Figure 2. The compressive component of the connection is identical to that used in conventional use of SDCL system.

EXPERIMENTAL PROGRAM

The experimental testing performed on the connection detail was identical to that used in the development of the SDCL system. Additional details of the original specimen design can be found elsewhere (Lampe et al., 2014; Azizinamini, Lampe and Yakel, 2003; Azizinamini et al., 2005).

Specimen Geometry

The test specimens represented a full-scale model of a portion of a bridge in service. The prototype bridge consists of two 95-ft continuous spans with four steel I-girders.

The test specimen represents the interior pier region of the two-span bridge, from inflection point to inflection point, as shown in Figure 3. Loads applied at the ends of the cantilevers allow simulation of the loading the structure would be subjected to in the field and result in similar shear and moment profiles.

The basic deck reinforcement was based on the empirical deck design provisions. The longitudinal steel includes #5 bars at 12-in. on center in the top layer and #4 bars at 12-in. on center in the bottom layer. The transverse reinforcement consists of #5 bars at 12-in. on center in the bottom layer and #4 bars at 12-in. on center in the top layer.

The negative moment produced by the live loads and superimposed dead loads is resisted by additional slab reinforcement at the pier location. The additional reinforcement required in the top layer is comprised of two #8 bars centered between adjacent #4 bars. Similarly, one #7 bar is centered between adjacent #5 bars in the bottom longitudinal

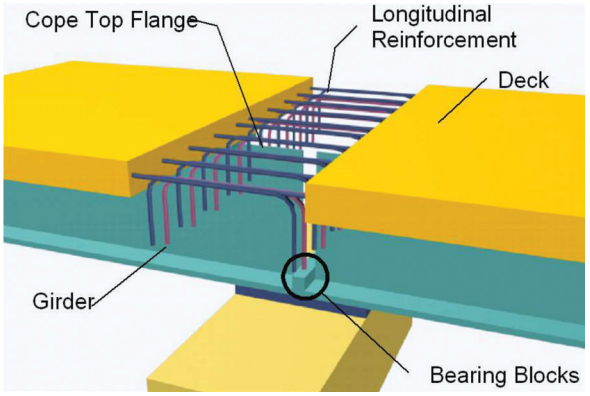

Fig. 2. Pier connection detail for modular system.

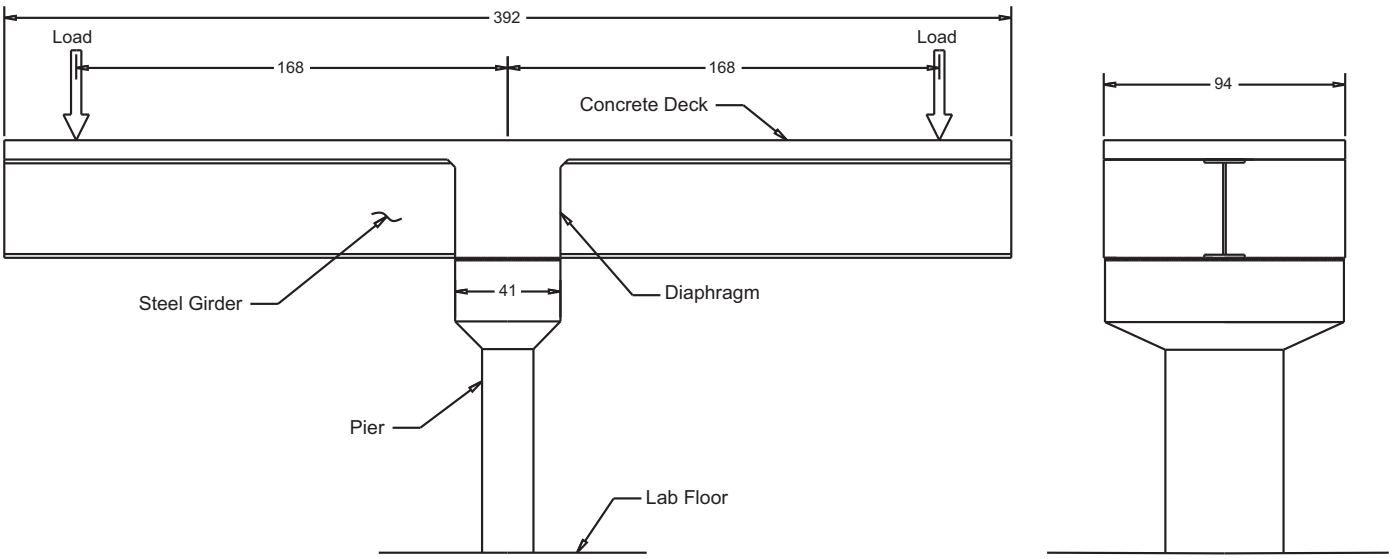

Fig. 3. Test specimen, dimensions in inches.

layer. This follows the typical two-thirds of the reinforcing steel in the top layer and one-third of the total area in the bottom layer. The details of the final slab reinforcement are shown in Figure 4. The L1, L2 and L3 notations indicate instrumentation locations and are discussed later.

To provide an additional resistance element in the connection, several high-strength bolts were attached to a region of the web located inside of the diaphragm. These bolts are shown in Figure 5. The results were inconclusive regarding the effectiveness of this detail. However, there is a need to prevent slippage of the girder web from the concrete diaphragm. The use of bolts as shown in Figure 5 is believed to accomplish this objective.

Because the test specimen is only a portion of the full bridge, it would have been unstable to cast the deck and then set the girders. Therefore, it was decided to build the specimen while the girders are in place on the pier. Although slightly different than the process to be used in the field, this change has no effect on the results of the study. Casting of the slab and diaphragm was completed in two stages. The first stage consisted of casting the diaphragm to half the total depth. This was done to add stability to the specimen during deck casting. The remainder of the diaphragm and the deck was cast 2 days later and was cured for 3 weeks.

Instrumentation

The specimen was monitored during the cyclic and ultimate tests using potentiometers, bonded electrical strain gages, welded and embedment vibrating wire strain gages, and a crack meter. Data were recorded through two data acquisition systems. Sixty-four resistance-based strain gages were mounted on the steel girders and longitudinal reinforcing bars to measure the strain variation during the test. Different parts of the girders, including top flange, bottom flange, web and bearing blocks, were instrumented by strain gages. Eleven vibrating wire embedment gages were used to monitor strain variations in the concrete diaphragm around the steel blocks in the longitudinal direction. A crack meter was installed between the girders' web at the centerline of the connection to measure the relative displacement of the two girders at both ends. Internal linear variable differential transformers (LVDTs) within the MTS rams measured the displacement of the specimen under the loading points during the cyclic test. Position transducers measured the displacement at two ends of the specimen during ultimate loading.

Materials

Twenty samples were cut from the steel rebar representing a sampling of all bar sizes. Figure 6 shows the engineering stress-strain curve for the #8 bars obtained from tensile tests. For the steel beam girders, samples were taken from near the end of the girder, which did not experience significant stress during testing. The average yield strength of the girder steel was determined to be 57 ksi, and the average ultimate stress was 72 ksi.

Concrete cylinders were prepared during the diaphragm and deck concrete casting. Based on the average compressive cylindrical test results, the 28-day compressive strength of the concrete was 5358 psi and 4947 psi for the deck and diaphragm, respectively.

Cyclic Testing

The bridge structure is expected to endure millions of cycles of repeated axle loads from vehicles during the design life. The available data show that the number of trucks on a bridge can reach more than 180 million vehicle load cycles during

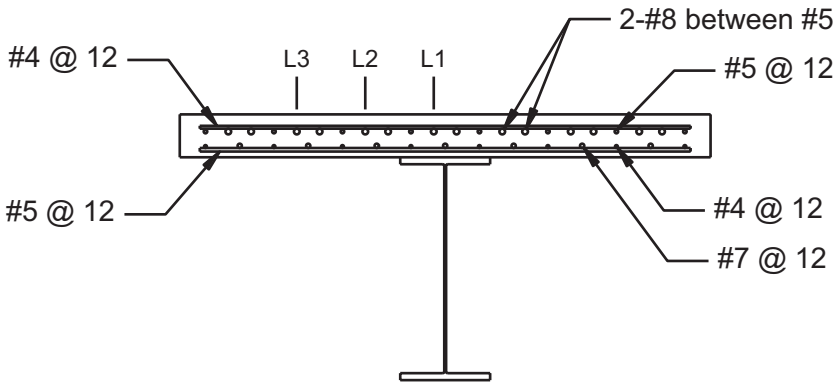

Fig. 4. Concrete slab section.

Fig. 5. Test specimen end detail.

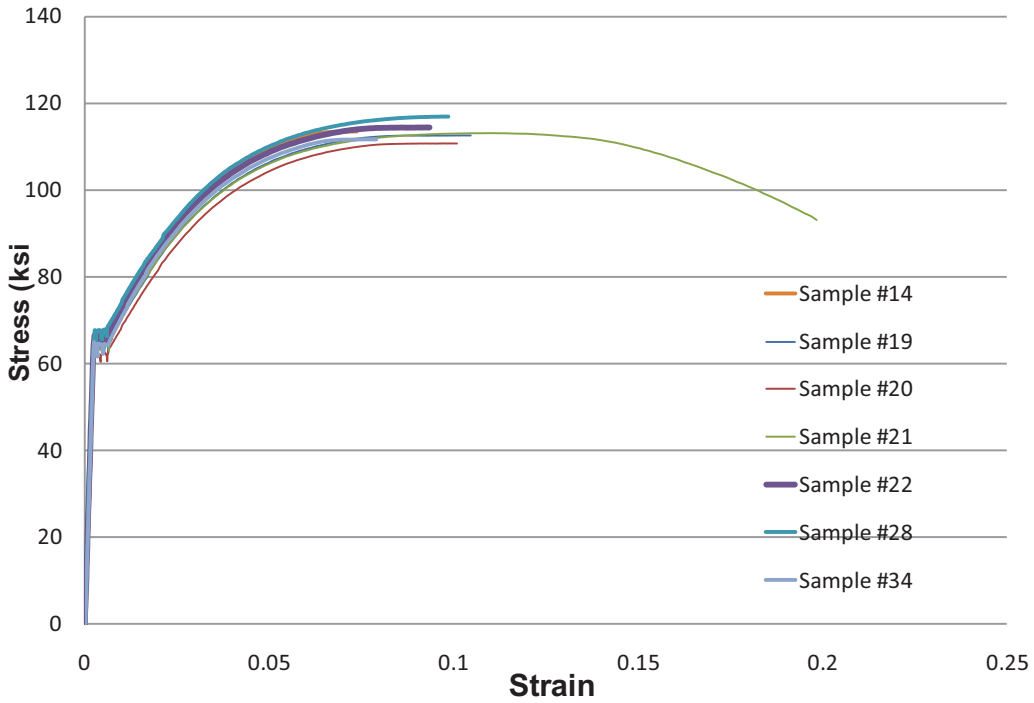

Fig. 6. Tensile test results for the #8 reinforcing bars.

the life time of 100 years (Szerszen and Nowak, 2000). The proposed connection should be able to operate and survive when subjected to cyclic loading generated by truck traffic. The specific goal of the cyclic testing performed was not intended to determine the fatigue strength or limit of the details, but rather as a proof loading to investigate whether the proposed details are capable of surviving a loading regimen equivalent to the cyclic loading anticipated over the design life of the bridge.

Procedure

The AASHTO *LRFD Bridge Design Specifications* (2007) were used to determine the fatigue resistance stress range based on the 75 years of service life for the bridge. During this period, the connection was expected to experience 135 million cycles. Applying this number of cycles would require an inordinate amount of time at a rate of two cycles per second. Therefore, the applied stress range was increased in order to reduce the number of cycles required to carry out the test. Four million cycles was chosen for the fatigue test. The applied moment for 4 million cycles to cause the same damage as 135 million cycles can be found by using the relationship developed herein and further explained in Lampe et al. (2014).

The fatigue limit state load combination was used to calculate the shear and moment envelope to which the prototype bridge would be subjected to. According to AASHTO-LRFD Specifications (1998), the prototype bridge, during its 75 year design life, and consequently, the connection of the two girders at the pier location, will experience 135,000,000 cycles of truck loadings. The simulation of this number of cycles in the laboratory would have taken a prohibitively long time. Therefore, there was a need to develop a procedure that could simulate 75 years of traffic in a reasonable time frame. This was accomplished by amplifying the level of load that was applied, as described later. Complete details of the procedure are provided in Lampe, Mossahebi, Yakel and Azizinamini (2013).

Equation 1 provides a relation between the loads and number of cycles under two conditions. Condition 1 represents the loading and number of cycles applied during the service life of the real structure as assumed for design. Condition 2 represents the structure under amplified loading.

$$\frac{M_1}{M_2} = \left(\frac{N_2}{N_1}\right)^{1/3} \tag{1}$$

where

M_1 = actual load
N_1 = cycles for actual structure corresponding to load of M_1
M_2 = amplified load (desired quantity)
M_2 = number of test cycles at load of M_1

From the bridge design calculations, the governing fatigue moment, M_1, is 352 kip-ft at an N_1 equal to 1.35 million cycles. With M_1 and N_1 known and having a desire to apply only 4 million cycles to reduce testing period (N_2 = 4,000,000 cycles), the applied moment needs to be increased to 1137 kip-ft as compared to 352 kip-ft. Given that the moment arm is 14 ft means 81 kips load must be applied to achieve the required moment (1137 ft-kips). In the laboratory, a 5-kip initial load was applied to the specimen and then the cyclic load was changed between 5 and 86 kips.

Two 1000-kN (220 kips) MTS actuators were used to apply the cyclic loading at 2 Hz (two cycles per seconds).

General Behavior of the Connection

Load-displacement curves for five periods during the cyclic test are generated at 1 million cycle intervals. Figures 7a and 7b show the load-displacement curves for the east and west side of the specimen, respectively.

Two observations can be made. First, there is a small difference between the stiffness of the west and east side of the connection. Second, it was observed that the initial load-displacement curve has a slightly greater slope than subsequent curves at later loading cycles. A 3.8% stiffness reduction was observed at the end of 4 million cycles.

Crack Pattern and Its Propagation on the Deck

No cracks were visible at the end of the curing period by visual inspection. After the initial application of load equivalent to the maximum fatigue load, the deck was again inspected and the initial cracks were mapped. During loading, the deck was inspected for cracking after each 1 million cycles. Figure 8 shows the crack map of the deck surface. The solid lines show the crack pattern after initial static load, while the dashed lines show the crack development during cycling. Note that the majority of crack growth occurred during the first 1 million cycles. No significant crack propagation was observed after 1 million cycles. As can be seen in the figure, little crack development occurred as a result of the cyclic loading. This would indicate that the connection performs well with regard to cracking of the concrete deck under repeated loading, which is important for the durability and service life of the structure.

Strain Profile in Longitudinal Direction

Six longitudinal reinforcing bars were instrumented to monitor the strain variation along the length of the bars. Figure 9 shows the strain variation along these six longitudinal bars, three on each side of the girder. Each figure is denoted by a name such as L1, which corresponds to the bar location as

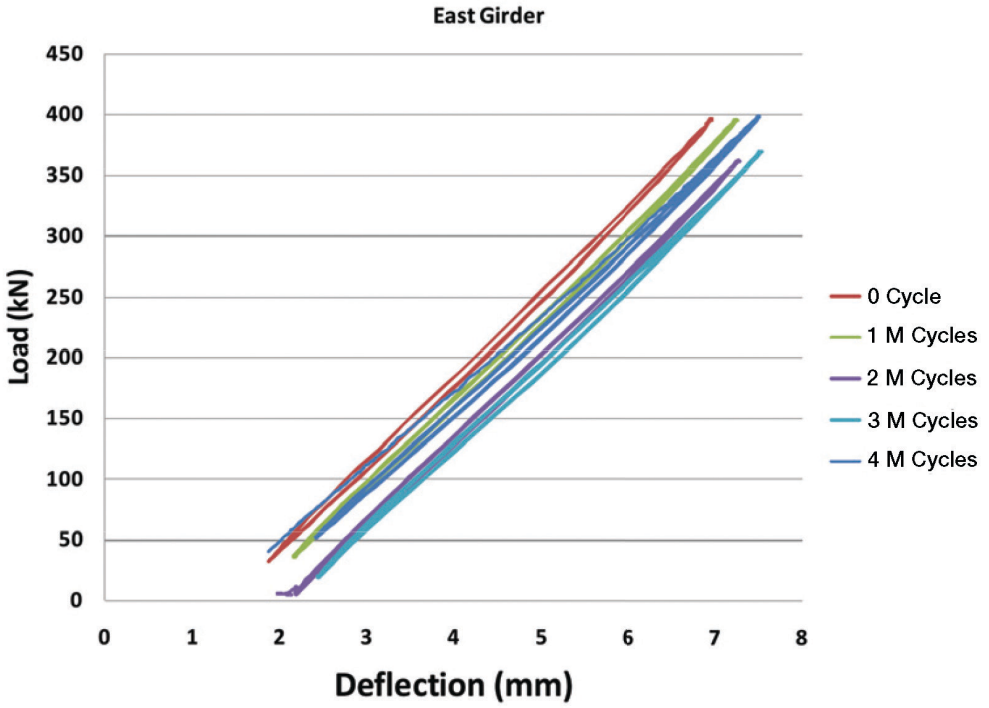

(a)

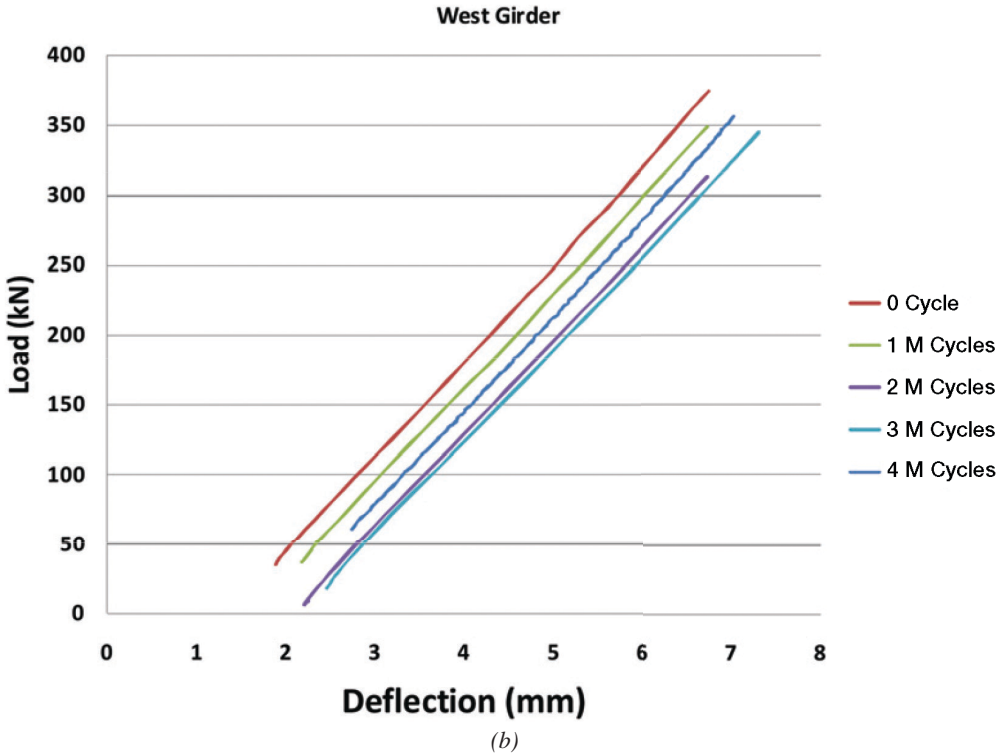

(b)

Fig. 7. Load-displacement curves for (a) the east side of the specimen and (b) the west side of the specimen.

shown in Figure 4. In all cases, the maximum strain occurs at point B, which is located just outside of the diaphragm. Longitudinal bars from each side lap each other in the diaphragm zone. Consequently, the area of longitudinal bars is doubled in this region, causing the bars to exhibit lower strain values than locations outside of the diaphragm region. The strain results in the longitudinal bars show that the bars are fully developed within the diaphragm region due in large part to presence of the hook.

The results show that the strain in the longitudinal bars increased slightly during the cyclic test. This change is more significant in the portion of deck outside of the diaphragm. The majority of this change happened within the first 1 million cycles. The average strain increase is 30 με, which is very small. The increase can be cracking in the deck. It can be concluded that performance of the connection was satisfactory during the fatigue service life.

Ultimate Test

The ultimate load test was carried out to investigate the behavior of the specimen under the ultimate load and evaluate the strength of the system. Loading of the specimen was achieved by placing a spreader beam on the deck at each end of the specimen. Threaded rods extended from the spreader to the basement of the structures laboratory, where they connected to hydraulic actuators. The loading system for the second test is shown in Figure 10. The distance of the spreader beam center to the centerline of the pier was 15 ft. During testing, displacement was applied in small increments with pauses for observations and data acquisition.

General Behavior of the Connection

Displacement was applied to the specimen until the specimen could no longer support additional load. The load-displacement curves were generated for both the west and east side of the connection and are shown in Figures 11 and 12, respectively. There is a slight difference in stiffness between the two ends. This is attributable to slight asymmetry or perturbations favoring one side of the connection. Other factors contributing to this slight difference could be unsymmetrical cracking in the deck concrete. The load corresponding to the theoretical plastic moment is shown in Figures 11 and 12. This calculation is based on the actual material properties and assumes complete participation of the full steel section and reinforcement. The assumption provides a value for reference and is not necessarily a basis for strength calculation, which is discussed in more detail elsewhere (Farimani et al., 2014).

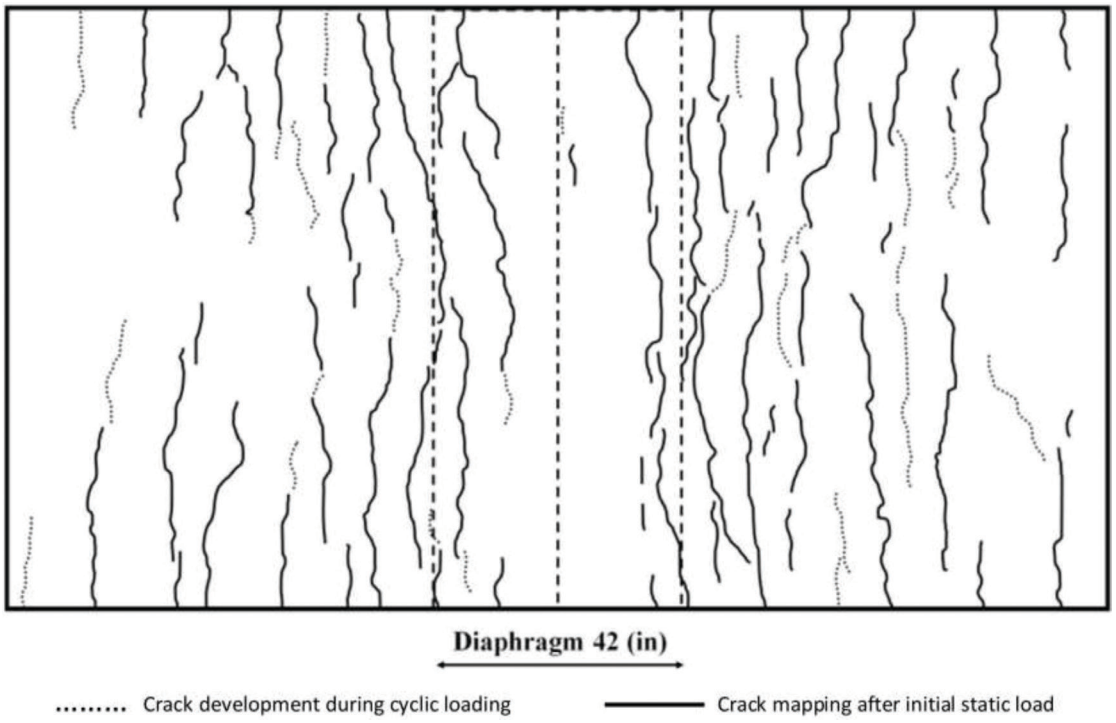

Fig. 8. Cracking on the slab deck surface.

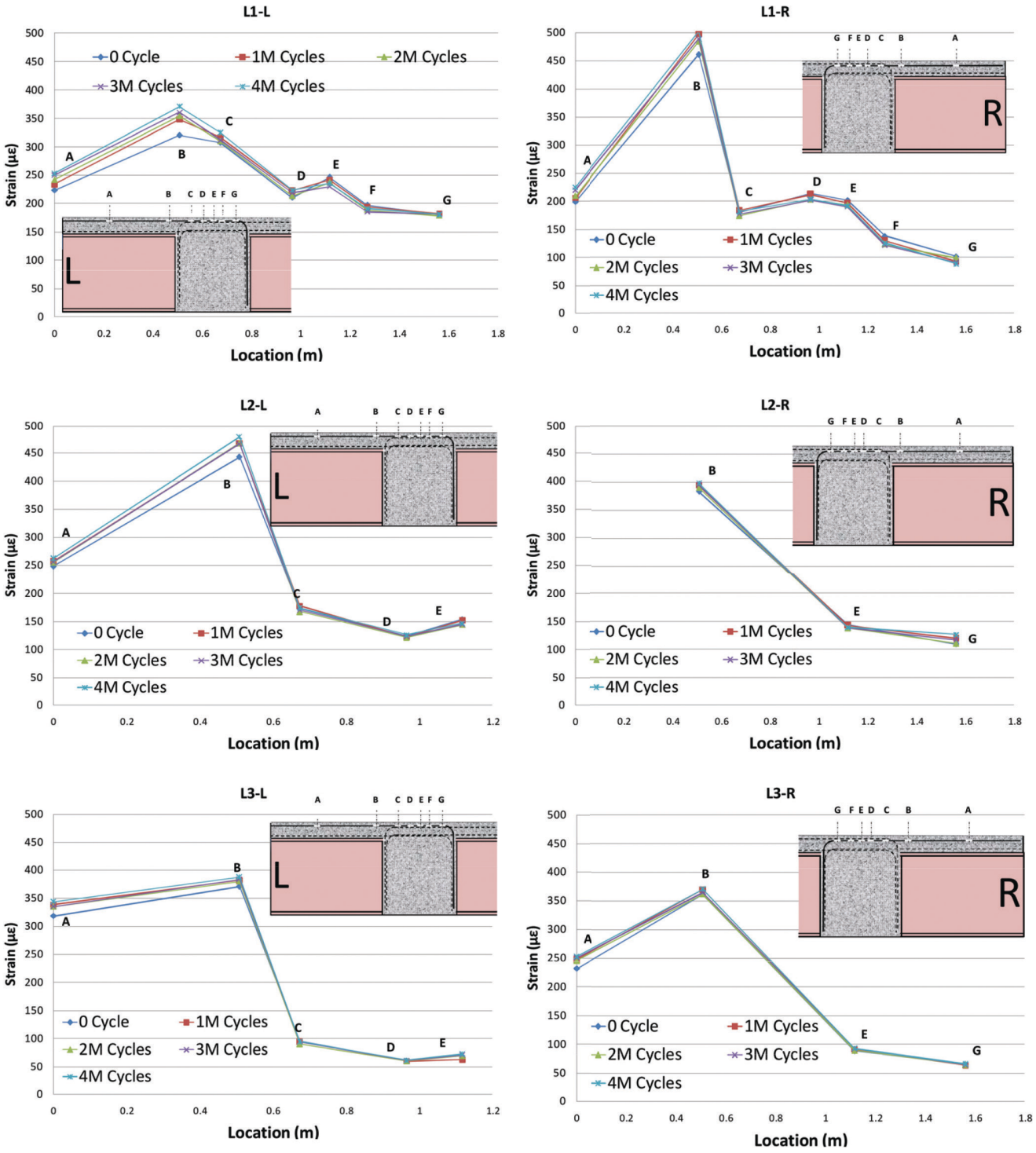

Fig. 9. Strain variation along the six longitudinal bars (L1-L, L1-R, L2-L, L2-R, L3-L, L3-R) during cyclic test.

The load-displacement behavior can be broken into four distinct regimens. At the outset of loading, there is a linear relation between the load and deflection. When the loading reached approximately 300 kips, this relation becomes nonlinear. This relationship can be seen in Figures 11 and 12 as a rounding of the load-displacement curve, corresponding to the initial yield of tension steel in the deck, over the pier. Once the majority of the tension steel over the pier has yielded, the behavior enters a plateau state, where there is little increase in load despite the application of large amounts of displacement. The small amount of load increase is mostly attributed to strain hardening of the tension steel. Note that the specimen was unloaded and reloaded several times during the test. Finally, at a load of approximately 415 kips and an applied displacement of 6.4 in., the load began dropping in response to the application of additional displacement, indicating the ultimate failure of the connection. Loading of the specimen continued until the end displacement of about 13 in. was achieved. The load corresponding to this displacement level (13 in.) was about 325 kips. This demonstrates the extreme ductility available from the connection. For the sake of clarity, the descending portions of the load displacement response of the test specimen are not shown in Figures 11 and 12.

Vertical Strain Profile in the Girders

Both girders were instrumented to monitor the strain variation during loading. The vertical strain profile was obtained at five locations, three locations in the west girder and two in the east girder. Figure 13 shows the vertical strain profile along the depth of the girder during ultimate loading for the various sections. The location of the strain gages and the section under the study are shown in each picture. The strain distribution along the depth of the girder is linear, and the location of the neutral axis based on the experimental results is in good agreement with that obtained theoretically. The strain distribution remained mostly linear through the test, the exceptions being the bottom flange on the west side just outside the diaphragm and the top flange on the east side just outside the diaphragm. It should be noted that these deviations from linearity were observed even at very low load levels and are, therefore, not a result of damage sustained during loading. However, the exact cause of these deviations was not identified.

Longitudinal Strain Profile in Continuity Reinforcement (Top Layer)

Longitudinal reinforcing bars were instrumented to monitor the strain variation along the length of the bars. Figure 14 shows the strain variation along bars at three different

Fig. 10. Ultimate test setup for the second test.

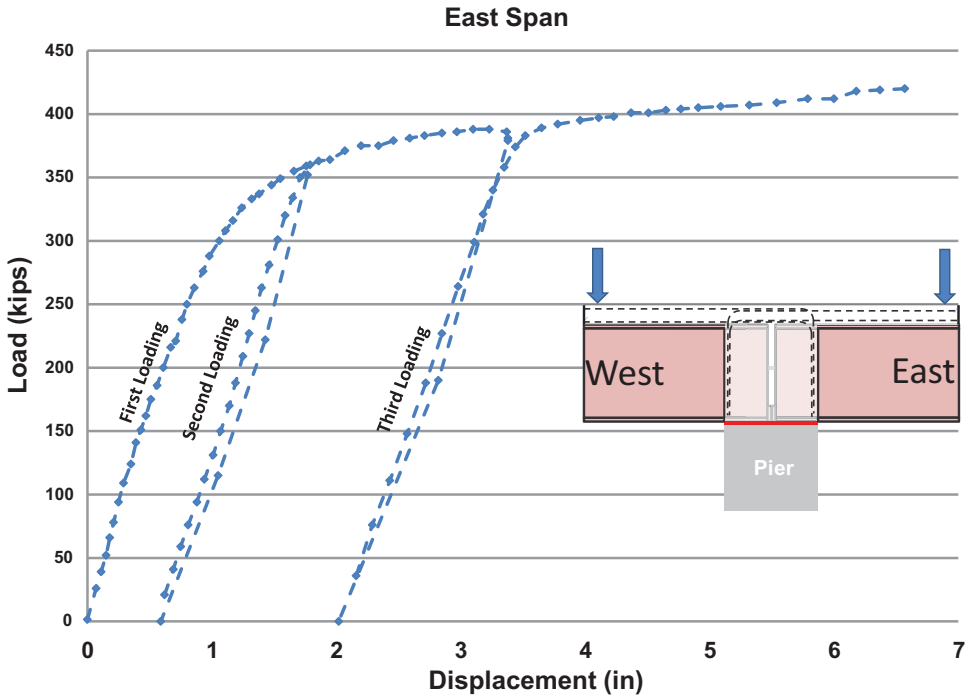

Fig. 11. Load displacement (east side).

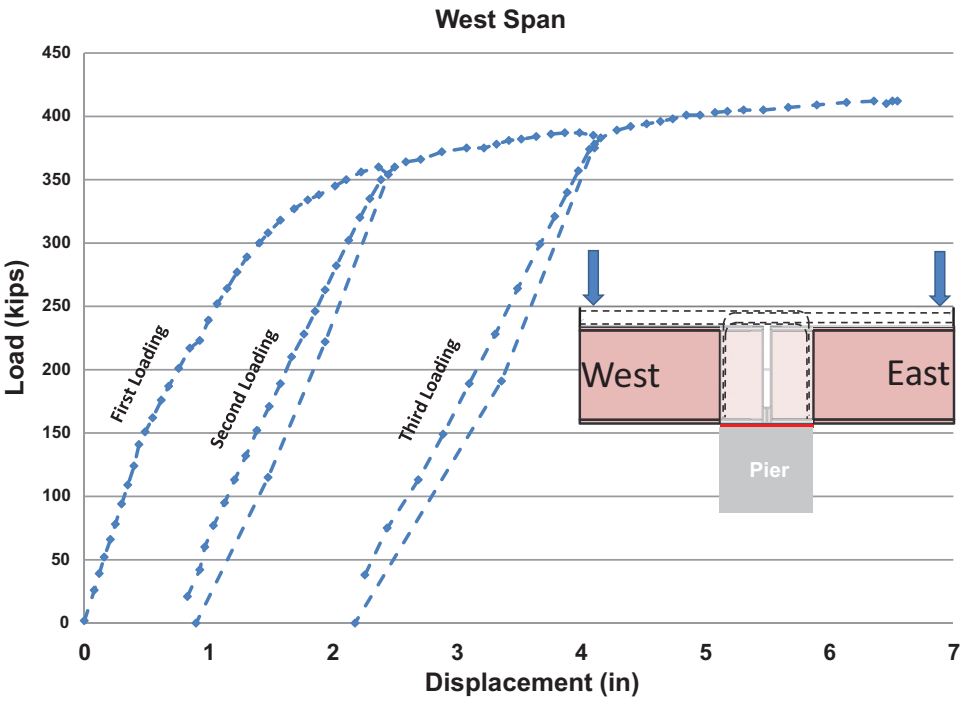

Fig. 12. Load displacement (west side).

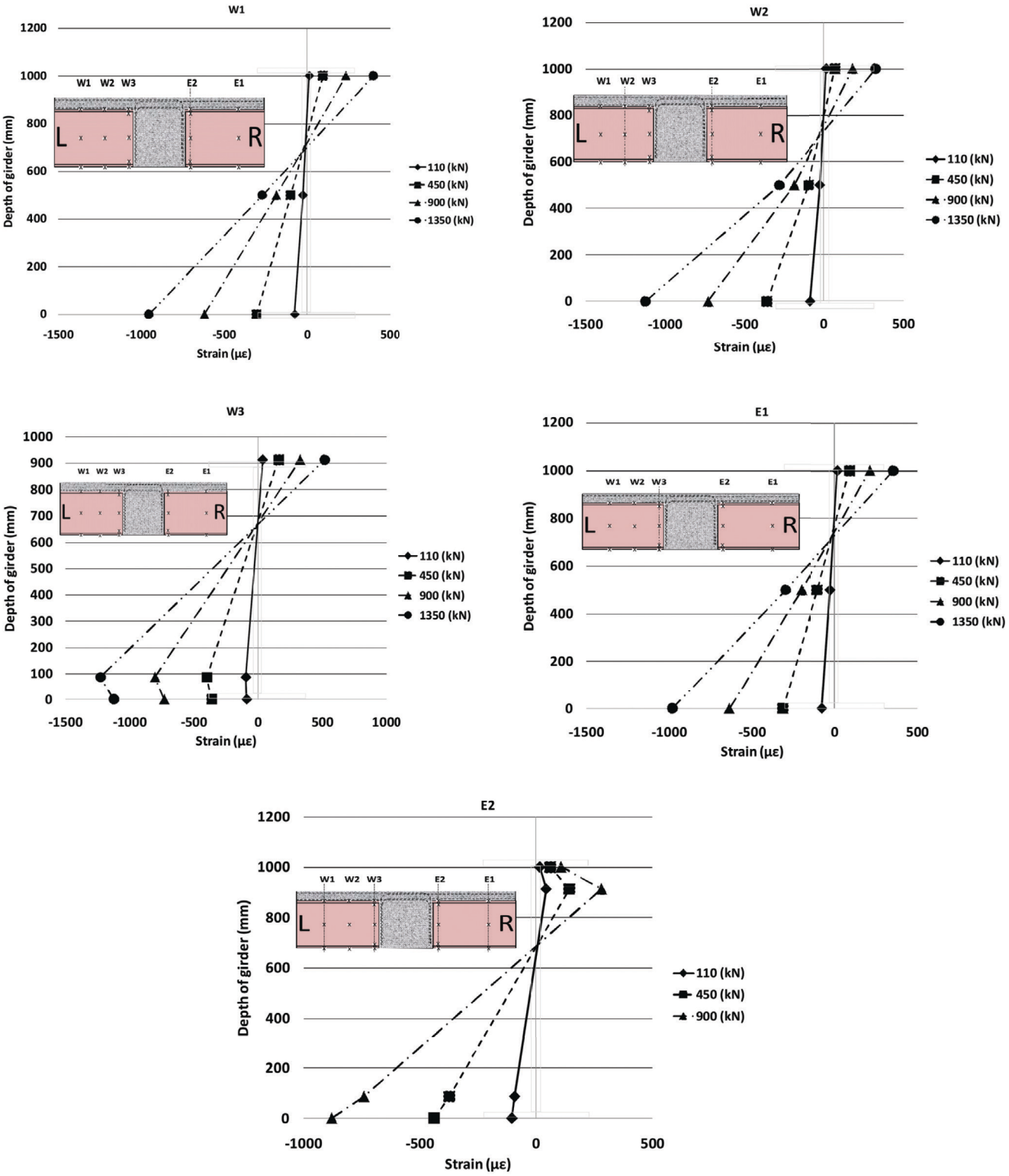

Fig. 13. Strain profile along the depth of the girder (W1, W2, W3, E1, E2) during ultimate load test.

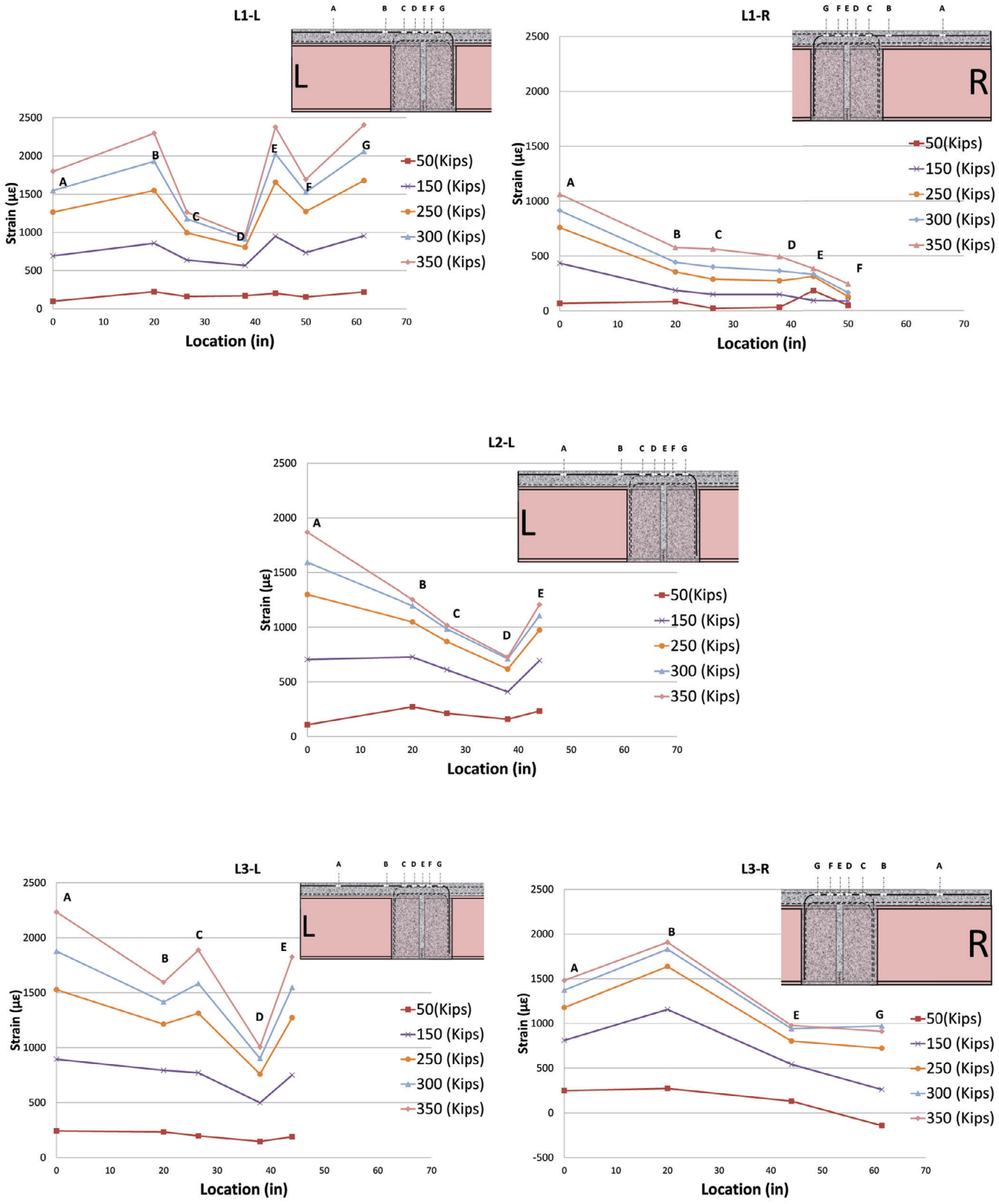

Fig. 14. Strain variation along the longitudinal bars (L1-L, L1-R, L2-L, L3-L, L3-R) during ultimate load test.

transverse positions. Because the bars are not continuous, each longitudinal rebar belongs to either the right or the left side of the specimen, which is indicated in the figure. Each figure is also denoted with a name such as L1, which corresponds to the bar location as shown in Figure 4. The strain variation observed in Figure 4 indicates that in general the strain decreases toward the hook end of each reinforcing bar developed using hooked end and splice. This behavior is mainly because the reinforcing bars over the pier are developed by splicing. This is a typical variation of strain over splice region (Azizinamini et al., 1999).

Separation at Centerline of Connection

A crack meter was installed between the girders to measure the separation during ultimate load. Figure 15 shows the displacement versus loading. As can be seen, no significant displacement was measured for loading up to 150 kips. A displacement equal to 0.2 in. was observed at the ultimate load.

Concrete Strain Variation in Diaphragm

The concrete strain variation in the region below the neutral axis and close to the steel blocks was monitored. Figure 16 shows the strain variation along the depth of the girder next to the web. The results show that there was no considerable strain at all monitored locations prior to 70 kips of applied load. Increasing the load beyond this value, the concrete began to exhibit some compressive strains in the lower region of the diaphragm. However, the gages indicate that the strains remained low, meaning the concrete was not significantly involved in the force transfer mechanism of this connection. For the most part, the compression force from one girder to another is transferred through the steel blocks welded to bottom portions of each girder.

Visual Inspection after Test Completion

Crack development was documented during the ultimate load test. The observation reported herein corresponds to condition of the test specimen at the conclusion of the testing. As mentioned earlier, the maximum load-carrying capacity of the test specimen was achieved when the end displacement was about 7 in. (see Figures 11 and 12), while loading was continued until end displacement of about 13 in. was achieved. This additional loading, beyond maximum loading capacity of the test specimen, resulted in significant additional damage to the test specimen.

Figure 17 shows the cracks that developed at test conclusion. The near side in the photograph is toward the east, which sustained much more damage than the west. As soon as one side begins to fail, the load drops; the other side may then never experience the same amount of damage.

APPLICATION OF THE SYSTEM

After the successful experimental test, this connection was used in construction of the 262nd Street Bridge over I-80 near Ashland, Nebraska. This type of connection can be employed in several different ways in conjunction with modular bridge construction. The adjacent beam concept used in the 262nd Street Bridge is one such example. The adjacent box concept utilizes prefabricated units consisting of an individual steel box girder topped by a portion of deck slab. These units are prefabricated and then shipped to the job site. Once on site, the individual units are set into place on two supports adjacent to one another. A longitudinal deck closure strip between the individual units is then cast, thereby joining them together. At the same time, the concrete diaphragm over the middle pier is cast, joining the adjacent pre-topped girders. The middle concrete diaphragm connects the adjacent spans and provides continuity between the spans for subsequent live loads.

This bridge incorporates several innovative concepts. The bridge uses a modular pre-topped steel box girder system, which allows much of the construction process to be performed prior to placing the girders. The bridge incorporates the simple for dead–continuous for live load system. The individual girders are simply supported while the pre-topped deck is placed. Once in place, the modular units are joined together such that resulting system is continuous for live load. The steel box girders utilize high-performance steel (HPS 70W) in a hybrid configuration, 70-ksi steel in the bottom flange and 50-ksi steel in the top flanges and webs. The use of high-performance steel combined with the simple for dead–continuous for live load system eliminates the need for section transitions through the length of the structure and uses constant cross-section throughout the length of the girders.

Figure 18 shows the cross-section of the bridge used for the 262nd Street Bridge. It consists of three pre-topped girders with vertical webs and two closure-pour regions, each 12 in. wide. The bottom flanges of the girder utilized 70-ksi high-performance steel with webs and top flanges using 50 ksi-steel.

Pre-topping the girder was performed on site, away from the final position of the girder. However, an alternative would be to pre-top the girder prior to shipping the girder to site. Figure 19 shows the layout of the pre-topped girder units.

Figure 20 shows the forming and casting of the deck for the pre-topped girders used for the 262nd Street Bridge, prior to placing them over the support.

A means was provided for lifting the pre-topped girders and placing them over the supports. Figure 21 shows the method used for lifting the pre-topped girders and placing them into their final positions; Figure 22 shows the lifting

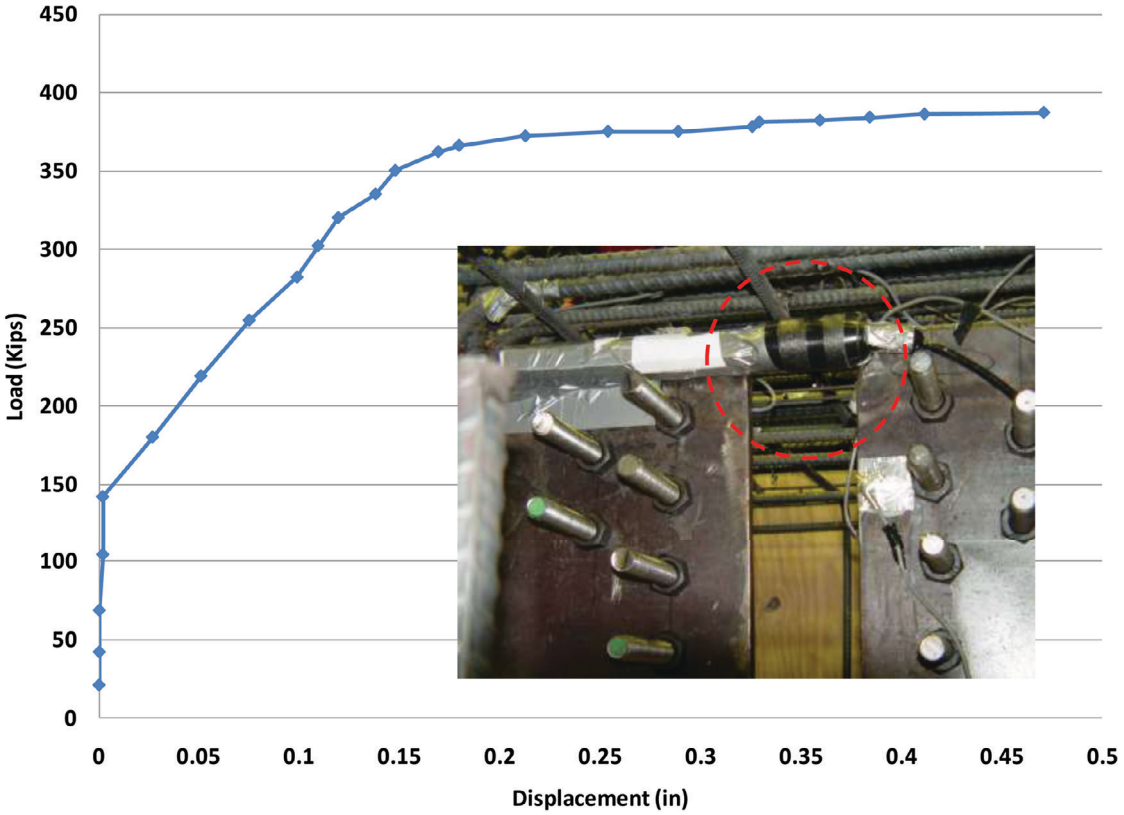

Fig. 15. Top flange separation.

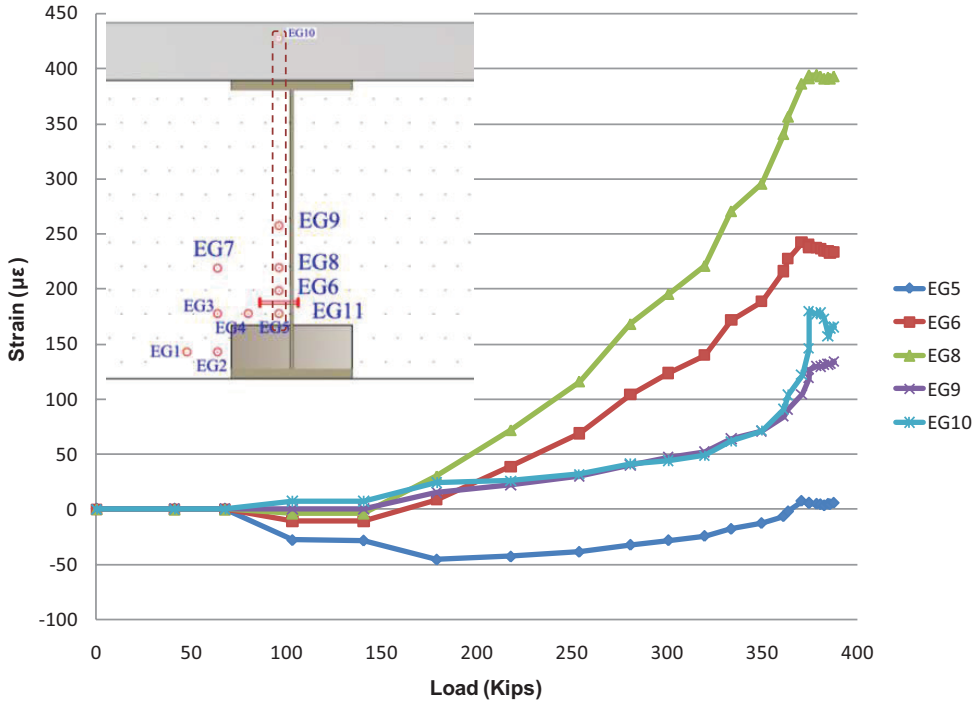

Fig. 16. Strain variation at concrete in vicinity of the steel blocks and web inside the diaphragm.

Fig. 17. Photo of specimen after conclusion of test.

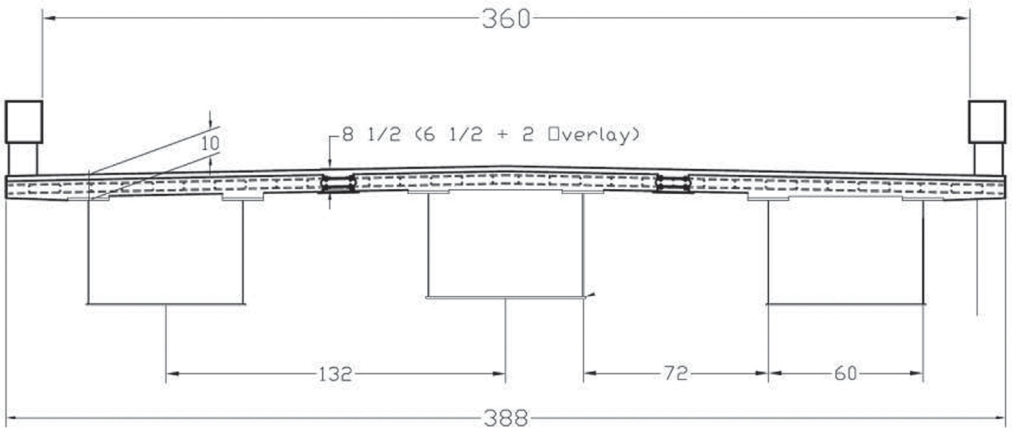

Fig. 18. Bridge cross-section consisting of three box girders.

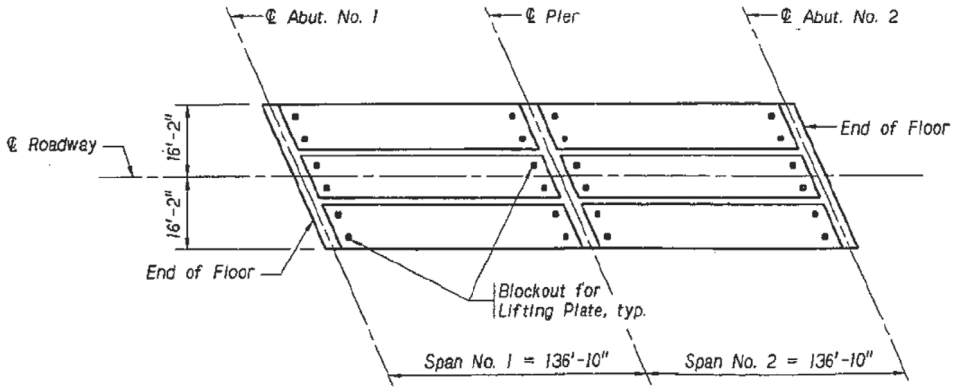

Fig. 19. Spanning and girder unit arrangement.

(a)

(b)

Fig. 20. Preparation of girder units for pre-topping operation: (a) forming; (b) reinforcement.

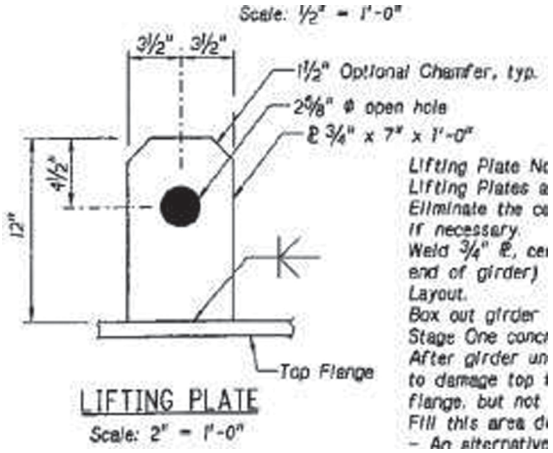

Fig. 21. Lifting of a single pre-topped girder for the 262nd Street Bridge.

Fig. 22. Second girder in second span of the 262nd Street Bridge.

operation of one of the girders, which was achieved using two cranes.

Adjacent girders have transverse reinforcement that extends beyond the slab edges. The adjacent pre-topped girders are connected through longitudinal closure pours. Figure 23 shows the alternative used for connecting the adjacent girders for the 262nd Street Bridge. The alternative shown in Figure 23, developed by the University of Texas (Thompson et al., 2003), consists of headed bars, which can provide development of the bars in short distances of only 8 in. Alternatively, ultra-high-performance concrete and regular reinforcing bars could be used in the longitudinal joint regions.

The chosen closure pour width was 12 in. Figure 24 shows the details of the closure pour and reinforcement. The detail over the pier used the detail described earlier in this paper (see Figures 1 and 2).

The sequence of completing the construction of the bridge depends on the depth of the pre-topped deck. There are two main alternatives. The pre-topped deck could be full or partial depth. The partial-depth alternative is attractive from the viewpoint of ensuring that the finished deck has the desired profile. When the partial-depth option is used, the construction sequence after placing the pre-topped deck units consists of casting the closure pour, casting the railing and finally placing the overlay. Because the 262nd Street Bridge was the first application where a modular steel bridge system was used incorporating several new ideas, the partial-deck option was selected as precautionary measure to allow minor adjustment, if needed. Figure 25 shows the view of

Fig. 23. Headed bar detail.

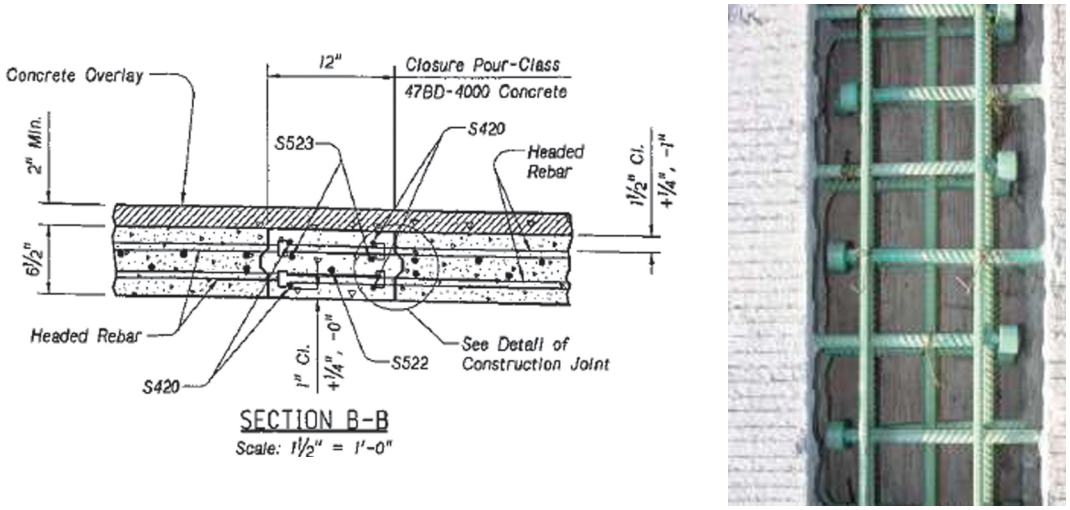

Fig. 24. Closure region details.

the 262nd Street Bridge after all of the pre-topped girders had been placed. The remaining operations were to cast the closure regions and then to apply the silica fume overlay.

MONITORING DATA

The instrumentation and monitoring of the 262nd Street Bridge was much more modest than the two previously reported bridge construction projects using the conventional SDCL system (Yakel and Azizinamini, 2014). With the basic performance of the SDCL system having been demonstrated, the focus was on the closure region performance. Figure 26 shows the representative instrumentation placed in the closure region. Additional gages were attached to the steel girders at the same location as the closure-pour instrumentation.

Figures 27 and 28 show the strain values obtained from the gages shown in Figure 26 both during the first 8 days of monitoring and also the full 21-month, long-term monitoring period. The results obtained indicate that the range of data is very limited, with no one gage showing a short-term variation greater than 100 με. The seasonal variation is also on the order of 100 με. These values are quite insignificant and indicate that the closure-pour region of the structure is not undergoing any long-term changes.

SUMMARY AND CONCLUSIONS

This paper presents a connection for use over the interior support of a continuous structure capable of extending the application of the simple for dead–continuous for live load steel bridge system (SDCL) to the case of accelerated bridge construction. The detail is intended to provide for use of the SDCL steel bridge system in conjunction with span-by-span construction of an adjacent pre-topped girder system. An experimental investigation was carried out to comprehend its performance followed by a field application, which was monitored for period of about 2 years.

The experimental investigation first examined the behavior of the detail under cyclic service-level loading. The performance of the connection was very good during the cyclic test. A 4% reduction of the connection stiffness was observed after simulating 100 years of truck traffic. This exceeds the typical design life of 70 years as specified by the AASHTO *LRFD Bridge Design Specifications* (2007). Specific observations through the testing include:

- Crack propagation was negligible through the cyclic test.
- No considerable change in the amount of strain in the longitudinal reinforcement was observed.

Fig. 25. Before casting the closure regions.

These observations demonstrate the capability of the system to develop the continuity reinforcement over the pier and maintain its integrity for 100 years of service life.

Following completion of the cyclic loading, the detail was monotonically loaded to failure. Specific observations made during the ultimate load test include:

- The connection displayed linear behavior until the applied load was sufficient to cause yielding of the longitudinal reinforcement.
- The connection reached its ultimate capacity after full yielding of longitudinal reinforcement had occurred.
- After yield, the connection demonstrated large displacement ductility before failure.

Further, examination of sensor data obtained from full-scale test indicated:

- The main element of the connection resisting the compression force was the steel block welded to the bottom portion of the end bearing plate.
- The contribution of the concrete in the vicinity of the steel block was small.
- The main element of the connection detail resisting the tension was the longitudinal continuity reinforcement within the deck.
- The connection failure coincided with tensile yielding of all longitudinal reinforcement within the full width of the deck.

The presented detail was used in the construction of the 262nd Street Bridge over I-80, near Ashland, Nebraska, which opened to traffic in October 2009. This bridge utilized adjacent, pre-topped, steel box-girders and the SDCL bridge system. The bridge consisted of two spans of three pre-topped steel-box units placed side by side. The side-by-side girders were connected using a longitudinal closure pour that developed headed reinforcement from the adjacent girders. The span-to-span connection over the pier was made using the details presented in this paper. After construction, the behavior of the structure was monitored continuously for a period of approximately 2 years, during which time it was observed that the behavior of the structure was essentially uniform, with only small seasonal fluctuations.

Based on the results of the experimental investigation and field trial, the SDCL steel bridge system using pre-topped adjacent girder units and the presented detail provide an economical and practical alternative bridge system suitable for accelerated bridge construction applications.

Fig. 26. Strain gages of closure in region 1.

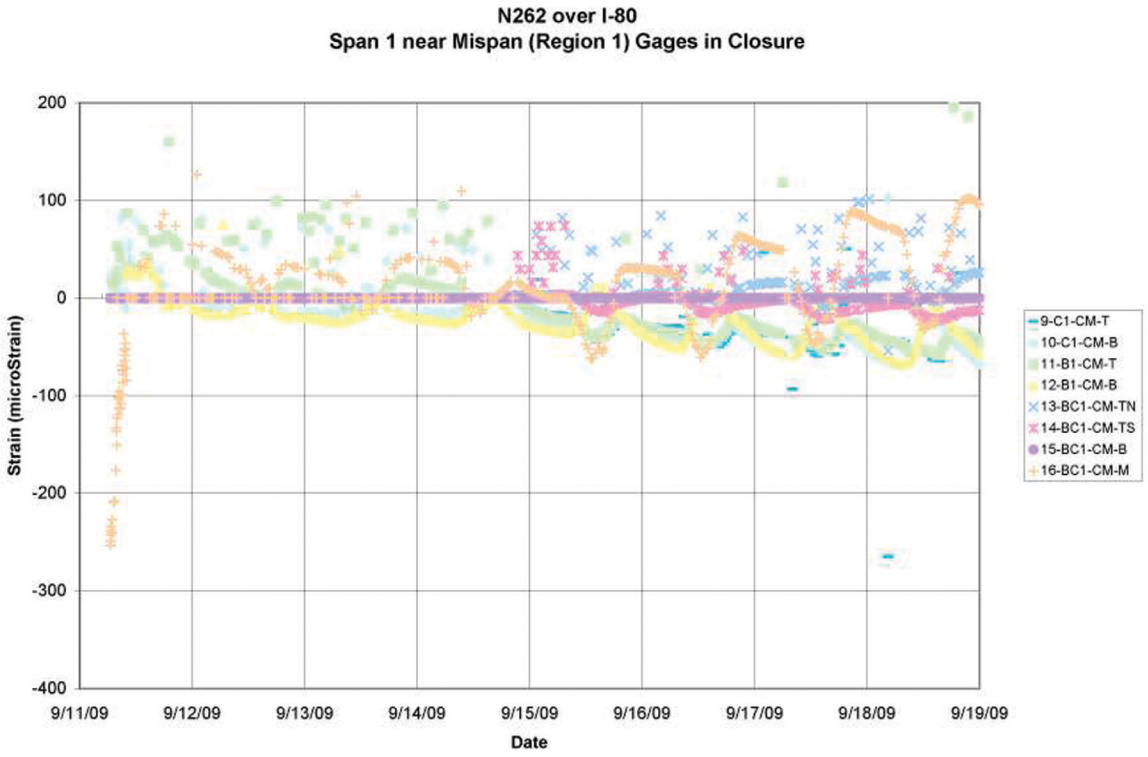

Fig. 27. Region 1 strains from closure gages (first 8 days).

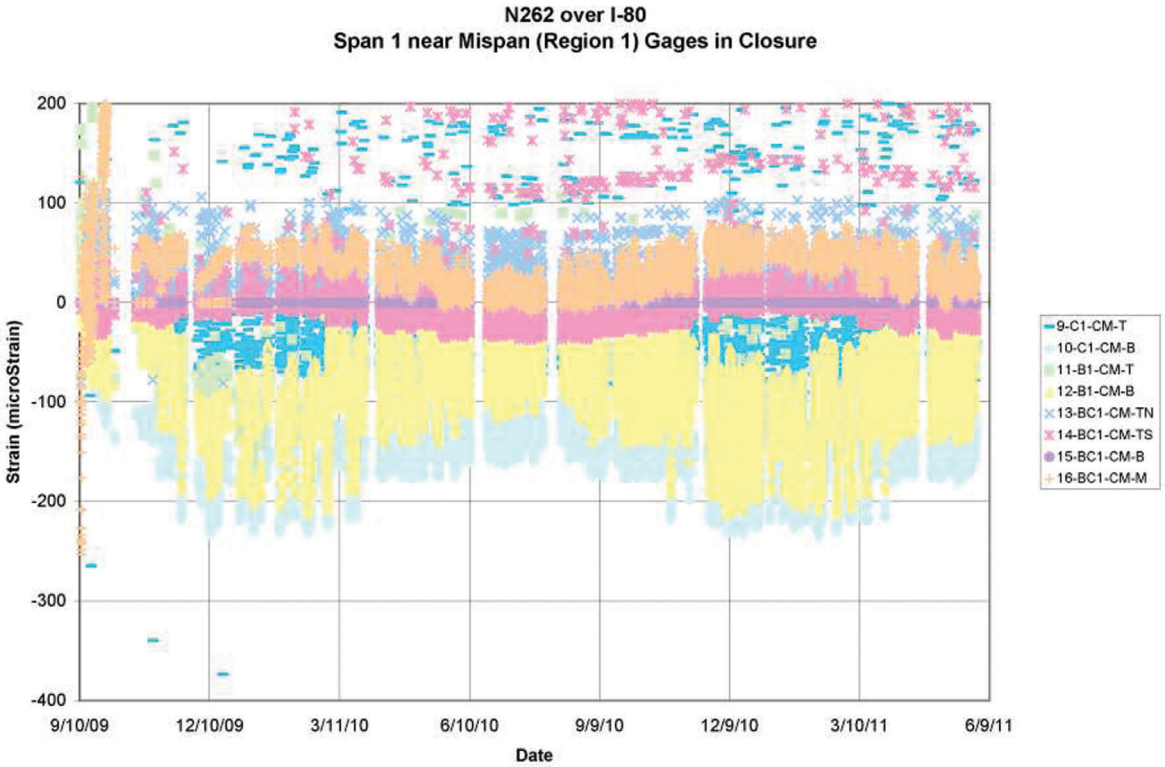

Fig. 28. Region 1 strains from closure gages (21 months).

ACKNOWLEDGMENTS

This paper presents details of a major undertaking to develop an economical steel bridge system. The investigation was directed by Dr. Atorod Azizinamini, Professor and Chair at Florida International University, and was made possible by contributions from many current and former graduate students and research associates, as well as input from many in the bridge community. In particular, the contributions of the following individuals are acknowledged.

Graduate students earning degrees from the project were Nick Lampe, Nazanin Mahasebi, Reza Farimani, Saeed Javidi, Derek Kowalski and Mark Otte. The research study was conducted at the University of Nebraska–Lincoln. Dr. Aaron Yakel was the research associate assisting the project. Laboratory technicians Jeff Boettcher, John Dageford, and Peter Hilsabeck assisted in conducting the experimental portion of the study. Graduate students who assisted with experimental testing include John Swendroski, J. Brian Hash, Patrick Mans, Luke Glaser and Nima Ala. The study was supported by the Federal Highway Administration and the Nebraska Department of Roads (NDOR). Several visionary engineers at NDOR were critical to the successful completion of the project: Mr. Lyman Freeman, Mr. Moe Jamshdi and Mr. Hussam "Sam" Fallaha. Steel fabrication and assistance during specimen preparation was provided by Capitol Contractors of Lincoln, Nebraska.

The opinions and conclusions presented in this paper are those of the authors and do not necessarily represent the viewpoints of the project sponsors.

REFERENCES

AASHTO (2007), *LRFD Bridge Design Specifications*, 4th ed., American Association of State Highway and Transportation Officials, Washington, DC.

Azizinamini, A. (2014), "Simple for Dead Load–Continuous for Live Load Steel Bridge Systems," AISC, *Engineering Journal*, Second Quarter, pp. 59–81.

Azizinamini, A., Lampe, N.J. and Yakel, A.J. (2003), *Toward Development of a Steel Bridge System—Simple for Dead Load and Continuous for Live Load*, A Final Report Submitted to the Nebraska Department of Roads, National Bridge Research Organization: http://www.nlc.state.ne.us/epubs/r6000/b016.0088-2003.pdf.

Azizinamini, A., Pavel, R., Hatfield, E., Ghosh, S.K. (1999), "Behavior of Lap-Spliced Reinforcing Bars Embedded in High-Strength Concrete," *ACI Structural Journal*, September–October, pp 826–835.

Azizinamini, A., Yakel, A.J., Lampe N.J., Mossahebi, N. and Otte, M. (2005), *Development of a Steel Bridge System—Simple for Dead Load and Continuous for Live Load, Volume 2: Experimental Results*, Final Report NDOR P542, Nebraska Department of Roads, Lincoln, NE, November.

Farimani, M.R., Javidi, S.N., Kowalski, D.T., Azizinamini, A. (2014), "Numerical Analysis and Design Provision Development for the Simple for Dead Load–Continuous for Live Load Steel Bridge System," AISC, *Engineering Journal*, Second Quarter, pp. 109–126.

Lampe, N.J., Mossahebi, N., Yakel, A.J., Farimani, M.R., and Azizinamini, A. (2014), "Development and Experimental Testing of Connections for the Simple for Dead Load–Continuous for Live Load Steel Bridge System," AISC, *Engineering Journal*, Second Quarter, pp. 83–108.

Szerszen, M.M. and Nowak, A. (2000), "Fatigue Evaluation of Steel and Concrete Bridges," *Transportation Research Record,* 1696.

Thompson, M.K., Ledesma, A.L., Jirsa, J.O., Breen, J.E. and Klingner, R.E. (2003), *Anchorage Behavior of Headed Reinforcement,* Center for Transportation Research Report 1855-3, Austin, Texas, May.

Yakel, A. J., and Azizinamini, A. (2014), "Field Application Case Studies and Long Term Monitoring of Bridges Utilizing the Simple for Dead–Continuous for Live Bridge System," *Engineering Journal*, AISC, Third Quarter, pp. 155–175.